

Syntheses, Crystal Structures, and Magnetic Properties of the Oxalato-Bridged Mixed-Valence Complexes $[\text{Fe}^{\text{II}}(\text{bpm})_3]_2[\text{Fe}^{\text{III}}_2(\text{ox})_5] \cdot 8\text{H}_2\text{O}$ and $\text{Fe}^{\text{II}}(\text{bpm})_3\text{Na}(\text{H}_2\text{O})_2\text{Fe}(\text{ox})_3 \cdot 4\text{H}_2\text{O}$ (bpm = 2,2'-Bipyrimidine)

Donatella Armentano,^{1a} Giovanni De Munno,^{*,1a} Juan Faus,^{1b} Francesc Lloret,^{1b} and Miguel Julve^{*,1b}

Dipartimento di Chimica, Università degli Studi della Calabria, 87030 Arcavacata di Rende, Cosenza, Italy, and Departament de Química Inorgànica, Facultat de Química de la Universitat de València, Avda. Dr. Moliner 50, 46100 Burjassot (València), Spain

Received March 7, 2000

The preparation and crystal structures of two oxalato-bridged $\text{Fe}^{\text{II}}-\text{Fe}^{\text{III}}$ mixed-valence compounds, $[\text{Fe}^{\text{II}}(\text{bpm})_3]_2[\text{Fe}^{\text{III}}_2(\text{ox})_5] \cdot 8\text{H}_2\text{O}$ (**1**) and $\text{Fe}^{\text{II}}(\text{bpm})_3\text{Na}(\text{H}_2\text{O})_2\text{Fe}(\text{ox})_3 \cdot 4\text{H}_2\text{O}$ (**2**) (bpm = 2,2'-bipyrimidine; ox = oxalate dianion) are reported here. Complex **1** crystallizes in the triclinic system, space group $P\bar{1}$, with $a = 10.998(2)$ Å, $b = 13.073(3)$ Å, $c = 13.308(3)$ Å, $\alpha = 101.95(2)^\circ$, $\beta = 109.20(2)^\circ$, $\gamma = 99.89(2)^\circ$, and $Z = 1$. Complex **2** crystallizes in the monoclinic system, space group $P2_1/c$, with $a = 12.609(2)$ Å, $b = 19.670(5)$ Å, $c = 15.843(3)$ Å, $\beta = 99.46(1)^\circ$, and $Z = 4$. The structure of complex **1** consists of centrosymmetric oxalato-bridged dinuclear high-spin iron(III) $[\text{Fe}_2(\text{ox})_5]^{2-}$ anions, tris-chelated low-spin iron(II) $[\text{Fe}(\text{bpm})_3]^{2+}$ cations, and lattice water molecules. The iron atoms are hexacoordinated: six oxygen atoms (iron(III)) from two bidentate and one bisbidentate oxalato ligands and six nitrogen atoms (iron(II)) from three bidentate bpm groups. The $\text{Fe}(\text{III})-\text{O}(\text{ox})$ and $\text{Fe}(\text{II})-\text{N}(\text{bpm})$ bond distances vary in the ranges 1.967(3)–2.099(3) and 1.967(4)–1.995(3) Å, respectively. The iron(III)–iron(III) separation across the bridging oxalato is 5.449(2) Å, whereas the shortest intermolecular iron(III)–iron(II) distance is 6.841(2) Å. The structure of complex **2** consists of neutral heterotrimeric $\text{Fe}(\text{bpm})_3\text{Na}(\text{H}_2\text{O})_2\text{Fe}(\text{ox})_3$ units and water molecules of crystallization. The tris-chelated low-spin iron(II) ($[\text{Fe}(\text{bpm})_3]^{2+}$) and high-spin iron(III) ($[\text{Fe}(\text{ox})_3]^{3-}$) entities act as bidentate ligands (through two bpm-nitrogen and two oxalato-oxygen atoms, respectively) toward the univalent sodium cation, yielding the trinuclear (bpm)₂Fe(II)–bpm–Na(I)–ox–Fe(III)–(ox)₂ complex. Two *cis*-coordinated water molecules complete the distorted octahedral surrounding of the sodium atom. The ranges of the $\text{Fe}(\text{II})-\text{N}(\text{bpm})$ and $\text{Fe}(\text{III})-\text{O}(\text{ox})$ bond distances [1.968(6)–1.993(5) and 1.992(6)–2.024(6) Å, respectively] compare well with those observed in **1**. The Na–N(bpm) bond lengths (2.548(7) and 2.677(7) Å) are longer than those of Na–O(ox) (2.514(7) and 2.380(7) Å) and Na–O(water) (2.334(15) and 2.356(12) Å). The intramolecular $\text{Fe}(\text{II}) \cdots \text{Fe}(\text{III})$ separation is 6.763(2) Å, whereas the shortest intermolecular $\text{Fe}(\text{II}) \cdots \text{Fe}(\text{II})$ and $\text{Fe}(\text{III}) \cdots \text{Fe}(\text{III})$ distances are 8.152(2) and 8.992(2) Å, respectively. Magnetic susceptibility measurements in the temperature range 2.0–290 K for **1** reveal that the high-spin iron(III) ions are antiferromagnetically coupled ($J = -6.6 \text{ cm}^{-1}$, the Hamiltonian being defined as $\hat{H} = -J\hat{S}_1 \cdot \hat{S}_2$). The magnitude of the antiferromagnetic coupling through the bridging oxalato in the magneto-structurally characterized family of formula $[\text{M}_2(\text{ox})_5]^{(2m-10)+}$ ($\text{M} = \text{Fe}(\text{III})$ (**1**), Cr(III), and Ni(II)) is analyzed and discussed by means of a simple orbital model.

Introduction

The tris-chelated $[\text{M}(\text{ox})_3]^{3-}$ complex ($\text{M} =$ trivalent first-row transition metal ion; ox = oxalate dianion) is a well-known ligand in the preparation of heterometallic complexes when using the so-called building block strategy.^{2–16} It has been found that its reaction with transition metal ions can lead to infinite

two- and three-dimensional magnetic networks depending on the nature of the templating cation. Therefore, honeycomb anionic layers of formula $[\text{M}^{\text{II}}\text{M}^{\text{III}}(\text{ox})_3]_n^{n-}$ ($\text{M}^{\text{II}} = \text{V}, \text{Cr}, \text{Mn}$,

- (1) (a) Università degli Studi della Calabria. (b) Universitat de València.
- (2) Pei, Y.; Journaux, Y.; Kahn, O. *Inorg. Chem.* **1989**, *28*, 100.
- (3) Tamaki, H.; Zhong, Z. J.; Matsumoto, N.; Kida, S.; Koikawa, M.; Achiwa, N.; Hashimoto, Y.; Okawa, H. *J. Am. Chem. Soc.* **1992**, *114*, 6974.
- (4) Atovmyan, L. O.; Shilov, G. V.; Lyubovskaya, R. N.; Zhilyaeva, E. I.; Ovanesyan, N. S.; Pirumova, S. I.; Gusakovskaya, I. G. *JETP Lett.* **1993**, *58*, 766.
- (5) Decurtins, S.; Schmalte, H. W.; Schneuwly, P.; Oswald, H. R. *Inorg. Chem.* **1993**, *32*, 1888.
- (6) Decurtins, S.; Schmalte, H. W.; Oswald, H. R.; Linden, A.; Ensling, J.; Gütllich, P.; Hauser, A. *Inorg. Chim. Acta* **1994**, *216*, 65.
- (7) Decurtins, S.; Schmalte, H. W.; Schneuwly, P.; Ensling, J.; Gütllich, P. *J. Am. Chem. Soc.* **1994**, *116*, 9521.

- (8) Reiff, W. M.; Kreis, J.; Meda, L.; Kirss, R. U. *Mol. Cryst. Liq. Cryst.* **1995**, *273*, 181.
- (9) Román, P.; Guzmán-Mirallas, C.; Luque, A. *J. Chem. Soc., Dalton Trans.* **1996**, 3985.
- (10) Mathonière, C.; Nuttall, C. J.; Carling, S. G.; Day, P. *Inorg. Chem.* **1996**, *35*, 1201.
- (11) Carling, S. G.; Mathonière, C.; Day, P.; Abdul Malik, K. M.; Coles, S. J.; Hursthouse, M. B. *J. Chem. Soc., Dalton Trans.* **1996**, 1839.
- (12) Decurtins, S.; Schmalte, H. W.; Pellaux, R.; Schneuwly, P.; Hauser, A. *Inorg. Chem.* **1996**, *35*, 1451.
- (13) Decurtins, S.; Schmalte, H. W.; Pellaux, R.; Huber, R.; Fischer, P.; Ouladdiaf, B. *Adv. Mater.* **1996**, *8*, 647.
- (14) Pellaux, R.; Schmalte, H. W.; Huber, R.; Fischer, P.; Hauss, T.; Ouladdiaf, B.; Decurtins, S. *Inorg. Chem.* **1997**, *36*, 2301.
- (15) Clemente-León, M.; Coronado, E.; Galán-Mascarós, J. R.; Gómez-Gracia, C. *J. Chem. Commun.* **1997**, 1727.
- (16) Hernández-Molina, M.; Lloret, F.; Ruiz-Pérez, C.; Julve, M. *Inorg. Chem.* **1998**, *37*, 4131.

Fe, Co, Ni, Cu, Zn; $M^{III} = V, Cr, Fe$) were synthesized by using bulky organic cations $[AX_4]^+$ ($A = N, P; X = \text{phenyl}, n\text{-alkyl}$)^{3,4,6,8,10,11,14} or decamethylferrocenium.¹⁵ Within each layer, the adjacent tris-chelated metal complexes exhibit different chirality. Given that at the six anionic layers present in the unit cell three have M^{III} in the Δ enantiomeric form and the other three only incorporate M^{III} in the λ conformation, the whole structure is not optically active. However, the 3D networks of formula $[M^{II}_2(\text{ox})_3]_n^{2n-}$, $[M^I M^{III}(\text{ox})_3]_n^{2n-}$, and $[M^I M^{III}(\text{ox})_3]_n^{n-}$ result when $[M(\text{bpy})_3]^{m+}$ ($\text{bpy} = 2,2'\text{-bipyridine}; m = 2 \text{ and } 3$) is used as counterion.^{5,7,9,12,13,16} In this latter case, the compound is chiral, both the cation and the anion being enantiomers. These chiral compounds were first prepared from the racemic starting materials, and only very recently, the feasibility of the enantioselective preparation of optically active two- and three-dimensional oxalate-bridged networks has been elegantly demonstrated using resolved $[\text{Cr}(\text{ox})_3]^{3-}$ and $[M(\text{bpy})_3]^{2+}$ ($M = \text{Ni, Ru}$) species.¹⁷

The remarkable ability of the oxalate ligand to mediate strong magnetic interactions between the metal ions^{18–21} makes these two- and three-dimensional oxalate-bridged networks valuable candidates for experimental and theoretical studies in the field of molecular-based magnets.^{22,23} However, the lack of suitable theoretical models to analyze these complex high-dimensional magnetic materials has so far precluded a thorough analysis of their magnetic properties. In the context of our magnetostructural studies concerning low-dimensionality systems with transition metal ions and bridging ligands such as oxalato and 2,2'-bipyrimidine (hereafter noted bpm),^{24–28} we have obtained the dinuclear $[\text{Fe}^{II}(\text{bpm})_3]_2[\text{Fe}^{III}_2(\text{ox})_5] \cdot 8\text{H}_2\text{O}$ (**1**) and trinuclear $\text{Fe}^{II}(\text{bpm})_3\text{Na}(\text{H}_2\text{O})_2\text{Fe}^{III}(\text{ox})_3 \cdot 4\text{H}_2\text{O}$ (**2**) complexes containing the high-spin $[\text{Fe}^{II}_2(\text{ox})_5]^{4-}$ (**1**) and $[\text{Fe}^{III}(\text{ox})_3]^{3-}$ (**2**) units and the low-spin $[\text{Fe}^{II}(\text{bpm})_3]^{2+}$ (**1** and **2**) entity. Their preparation, crystal structure characterization, and magnetic properties are presented here.

Experimental Section

Materials. Sodium and ammonium oxalate salts, iron(III) ammonium sulfate dodecahydrate, and 2,2'-bipyrimidine were purchased from

commercial sources and used as received. Elemental analyses (C, H, N) were performed by the Microanalytical Service of the Università degli Studi della Calabria. Iron content was determined by atomic absorption spectrometry.

Preparation of $[\text{Fe}(\text{bpm})_3]_2[\text{Fe}_2(\text{ox})_5] \cdot 8\text{H}_2\text{O}$ (1**) and $\text{Fe}(\text{bpm})_3\text{Na}(\text{H}_2\text{O})_2\text{Fe}(\text{ox})_3 \cdot 4\text{H}_2\text{O}$ (**2**).** Complex **1**, as red-brown plates, can be prepared (yield about 80%) by slow evaporation of aqueous solutions (50 mL) containing iron(III) ammonium sulfate dodecahydrate (or iron(III) chloride) (0.5 mmol), ammonium oxalate (1 mmol), and 2,2'-bipyrimidine (1.0 mmol). The crystals were filtered off and dried on filter paper in air. Compound **2** (red-brown parallelepipeds) was obtained as a minor product (yield of about 5%) together with compound **1** (yield of about 70%) from an aqueous solution (50 mL) containing sodium oxalate (1.0 mmol), iron(III) ammonium sulfate dodecahydrate (0.5 mmol), and bpm (0.5 mmol) by slow evaporation at room temperature. They were filtered off, dried on filter paper, and separated by hand. Anal. Calcd for $\text{C}_{58}\text{H}_{52}\text{Fe}_4\text{N}_{24}\text{O}_{28}$ (**1**): C, 39.66; H, 2.98; N, 19.14; Fe, 12.72. Found: C, 39.55, H, 3.02; N, 19.21; Fe, 12.68. Anal. Calcd for $\text{C}_{30}\text{H}_{30}\text{Fe}_2\text{N}_{12}\text{NaO}_{18}$ (**2**): C, 36.72; H, 3.08; N, 17.13; Fe, 11.38. Found: C, 36.68, H, 3.12; N, 17.09; Fe, 11.30.

The infrared spectrum of **1** reveals the presence of chelating bpm (doublet at 1578 and 1567 cm^{-1})²⁹ and chelating and bridging oxalato [1710, 1680, and 1630 cm^{-1} for $\nu_{\text{as}}(\text{O}-\text{C}-\text{O})$; 1357, 1310, 1240, and 873 cm^{-1} for $\nu_{\text{s}}(\text{O}-\text{C}-\text{O})$; 810 and 795 cm^{-1} for $\delta(\text{O}-\text{C}-\text{O})$].^{18b,21,30–32} The infrared spectrum of **2** shows chelating and bridging bpm (triplet at 1590, 1577, and 1551 cm^{-1}) and oxalato (1718, 1680, 1645, 1380, 1273, 1250, 895, 804, and 790 cm^{-1}). The presence of a strong and broad absorption at ca. 3420 cm^{-1} in the infrared spectra of **1** and **2** is indicative of the presence of hydrogen-bonded water molecules in these complexes.³³ All these spectral suggestions have been confirmed by the X-ray structural determinations of **1** and **2**.

Physical Techniques. The IR spectra of **1** and **2** were registered in solid KBr pellet on a Perkin-Elmer 1750 FTIR spectrophotometer, in the 4000–400 cm^{-1} region. Magnetic susceptibility measurements were performed on a polycrystalline sample of **1** with a Quantum Design superconducting quantum interference device (SQUID) magnetometer (2.0–300 K temperature range) using an applied magnetic field of 0.1 T. The susceptometer was calibrated with $(\text{NH}_4)_2\text{Mn}(\text{SO}_4)_2 \cdot 12\text{H}_2\text{O}$. The experimental susceptibility data of **1** were corrected for the diamagnetism estimated from Pascal's constants³⁴ [$-857 \times 10^{-6} \text{ cm}^3 \text{ mol}^{-1} \text{ K}$].

X-ray Data Collection and Structure Refinement. The diffraction data were collected at room temperature on a Bruker R3m/V automatic four-circle diffractometer using graphite monochromated Mo $K\alpha$ radiation ($\lambda = 0.71073 \text{ \AA}$) with the $\omega-2\theta$ scan method. The unit cell parameters were determined from least-squares refinement of the setting angles of 25 reflections in the 2θ range, 15–30°. Information concerning crystallographic data collection and structure refinements is summarized in Table 1. Examination of two standard reflections, monitored after every 98 reflections, showed no sign of crystal deterioration. Lorentz polarization and semiempirical (ψ scan) absorption corrections³⁵ were applied to the intensity data. The maximum and minimum transmission factors were 0.860 and 0.792 for **1** and 0.693 and 0.608 for **2**.

The structures were solved by standard Patterson methods and subsequently completed by Fourier recycling. All non-hydrogen atoms were refined anisotropically except for the oxygen atoms of the water

- (17) Andrés, R.; Gruselle, M.; Malézieux, B.; Verdager, M.; Vaissermann, J. *Inorg. Chem.* **1999**, *38*, 4637.
 (18) (a) Julve, M.; Verdager, M.; Gleizes, A.; Philoche-Levisalles, M.; Kahn, O. *Inorg. Chem.* **1984**, *23*, 3808. (b) Alvarez, S.; Julve, M.; Verdager, M. *Inorg. Chem.* **1990**, *29*, 4500. (c) Gleizes, A.; Julve, M.; Verdager, M.; Real, J. A.; Faus, J.; Solans, X. *J. Chem. Soc., Dalton Trans.* **1992**, 3209.
 (19) Ohba, M.; Tamaki, H.; Matsumoto, N.; Okawa, H. *Inorg. Chem.* **1993**, *32*, 5385.
 (20) Glerup, J.; Goodson, P. A.; Hodgson, D. J.; Michelsen, K. *Inorg. Chem.* **1995**, *34*, 6255.
 (21) Román, P.; Guzmán-Mirallas, C.; Luque, A.; Beitia, J. I.; Cano, J.; Lloret, F.; Julve, M.; Alvarez, S. *Inorg. Chem.* **1996**, *35*, 3741.
 (22) Decurtins, S.; Schmalte, H. W.; Pellaux, R.; Fischer, P.; Hauser, A. *Mol. Cryst. Liq. Cryst.* **1997**, *305*, 227.
 (23) Day, P. In *Supramolecular Engineering of Synthetic Metallic Materials*; Veciana, J.; Rovira, C.; Amabilino, D. B., Eds.; NATO ASI Series C518; Kluwer: Dordrecht, 1999; p 253.
 (24) De Munno, G.; Lloret, F.; Julve, M. In *Magnetism: A Supramolecular Function*; Kahn, O., Ed.; NATO ASI Series C484; Kluwer: Dordrecht, 1996; p 555.
 (25) De Munno, G.; Julve, M. In *Metal Ligand Interactions. Structure and Reactivity*; Russo, N.; Salahub, D., Eds.; NATO ASI Series C474; Kluwer: Dordrecht, 1996; p 139.
 (26) (a) De Munno, G.; Ruiz, R.; Lloret, F.; Faus, J.; Sessoli, R.; Julve, M. *Inorg. Chem.* **1995**, *34*, 408. (b) Curély, J.; Lloret, F.; Julve, M. *Phys. Rev. B* **1998**, *58*, 11465.
 (27) (a) De Munno, G.; Ventura, W.; Viau, G.; Lloret, F.; Faus, J.; Julve, M. *Inorg. Chem.* **1998**, *37*, 1458. (b) Sletten, J.; Daraghme, H.; Lloret, F.; Julve, M. *Inorg. Chim. Acta* **1998**, *279*, 127.
 (28) De Munno, G.; Armentano, D.; Julve, M.; Lloret, F.; Lescouëzec, R.; Faus, J. *Inorg. Chem.* **1999**, *38*, 2234.

- (29) Julve, M.; Verdager, M.; De Munno, G.; Real, J. A.; Bruno, G. *Inorg. Chem.* **1993**, *32*, 795.
 (30) Fujita, A. E.; Martell, A. E.; Nakamoto, K. *J. Phys. Chem.* **1962**, *36*, 324.
 (31) (a) Curtis, N. F. *J. Chem. Soc. A* **1968**, 1584. (b) Curtis, N. F. *J. Chem. Soc.* **1963**, 4109.
 (32) Masters, V. N.; Sharrad, C. A.; Bernhardt, P. V.; Gahan, L. G.; Moubaraki, B.; Murray, K. S. *J. Chem. Soc., Dalton Trans.* **1998**, 413.
 (33) Nakamoto, K. *Infrared and Raman Spectra of Inorganic and Coordination Compounds*, 4th ed.; Wiley: New York, 1986; p 227.
 (34) Earnshaw, A. *Introduction to Magnetochemistry*; Academic Press: London and New York, 1968.
 (35) North, A. C. T.; Philips, D. C.; Mathews, F. S. *Acta Crystallogr.* **1968**, *A24*, 351.

Table 1. Summary of Crystal Data^a for [Fe(bpm)₃]₂[Fe₂(ox)₅]·8H₂O (**1**) and Fe(bpm)₃Na(H₂O)Fe(ox)₃·4H₂O (**2**)

	1	2
formula	C ₅₈ H ₅₂ Fe ₄ N ₂₄ O ₂₈	C ₃₀ H ₃₀ Fe ₂ N ₁₂ NaO ₁₈
mol wt	1756.6	981.4
cryst syst	triclinic	monoclinic
space group	<i>P</i> 1	<i>P</i> 2 ₁ / <i>c</i>
<i>a</i> , Å	10.998(2)	12.609(2)
<i>b</i> , Å	13.073(3)	19.670(5)
<i>c</i> , Å	13.308(3)	15.843(3)
α , deg	101.95(2)	
β , deg	109.20(2)	99.46(1)
γ , deg	99.89(2)	
<i>V</i> , Å ³	1707.2(6)	3876(1)
<i>Z</i>	1	4
<i>D</i> _c , Kg m ⁻³	1.709	1.682
<i>F</i> (000)	896	2004
μ (Mo K α), cm ⁻¹	9.40	8.54
reflns, unique/observed	7494/4514	8501/5612
<i>R</i> ^b	0.048	0.085
<i>R</i> _w	0.074 ^c (all data)	0.251 ^d (all data)
<i>S</i>	1.256 ^e	1.046 ^f

^a Details in common: *T* = 25 °C, *I* > 3 σ (*I*) (**1**), *I* > 2 σ (*I*) (**2**). ^b *R* = $\sum(|F_o| - |F_c|)/\sum|F_o|$. ^c *R*_w = $[\sum w(|F_o| - |F_c|)^2/\sum w|F_o|^2]^{1/2}$. ^d *R*_w = $[\sum w(F_o^2 - F_c^2)^2/\sum w(F_o^2)^2]^{1/2}$. ^e Goodness of fit = $[\sum w(|F_o| - |F_c|)^2/(N_o - N_p)]^{1/2}$. ^f Goodness of fit = $[\sum w(F_o^2 - F_c^2)^2/(N_o - N_p)]^{1/2}$.

molecules of compound **2**. The hydrogen atoms of the bpm were set in calculated positions and refined as riding atoms with a common fixed isotropic thermal parameter. The hydrogen atoms of the water molecules (except those of **2**) were located on a ΔF map and refined with constraints. The refinement was performed on *F* (**1**) and *F*² (**2**) using 4514 for **1** and all 8501 reflections for **2**. The residual maxima and minima in the final Fourier difference maps were 0.59 and -0.44 for **1** and 1.66 and -0.60 for **2**. The nonoptimal refinement of compound **2** is related to the disorder of the water molecules. Solutions and refinements were performed with the SHELXTL PLUS and SHELXTL NT systems.³⁶ The final geometrical calculations were carried out with the PARST program.³⁷ The graphical manipulations were performed using the XP utility of the SHELXTL PLUS and SHELXTL NT systems. The main interatomic bond distances and angles are listed in Tables 2 (**1**) and 3 (**2**).

Results and Discussion

Description of the Structures. [Fe(bpm)₃]₂[Fe₂(ox)₅]·8H₂O (**1**). The structure of compound **1** consists of centrosymmetric dinuclear [Fe₂(ox)₅]⁴⁻ anions (Figure 1, top), mononuclear [Fe(bpm)₃]²⁺ cations (Figure 1, bottom) and crystallization water molecules linked together by means of electrostatic interactions and hydrogen bonds.

The anionic unit contains two Fe(III) atoms and four terminal and one bridging oxalato ligands. Each iron(III) ion has a distorted octahedral environment. The iron-to-bridging-oxalato bond lengths are significantly longer than those involving the terminal oxalato ligands as observed in the parent [Cr₂(ox)₅]⁴⁻ and [Ni₂(ox)₅]⁶⁻ anionic complexes.^{21,32} The mean value of the Fe(2)–O(terminal oxalate) bond lengths is comparable to the mean distance observed in X₃Fe(ox)₃·3H₂O with X = K⁺ (2.037 Å),³⁸ NH₄⁺ (2.002 Å),³⁹ and Rb⁺ (1.963 Å).⁴⁰ The iron atom is shifted by 0.072(2) Å from the best equatorial plane, which is

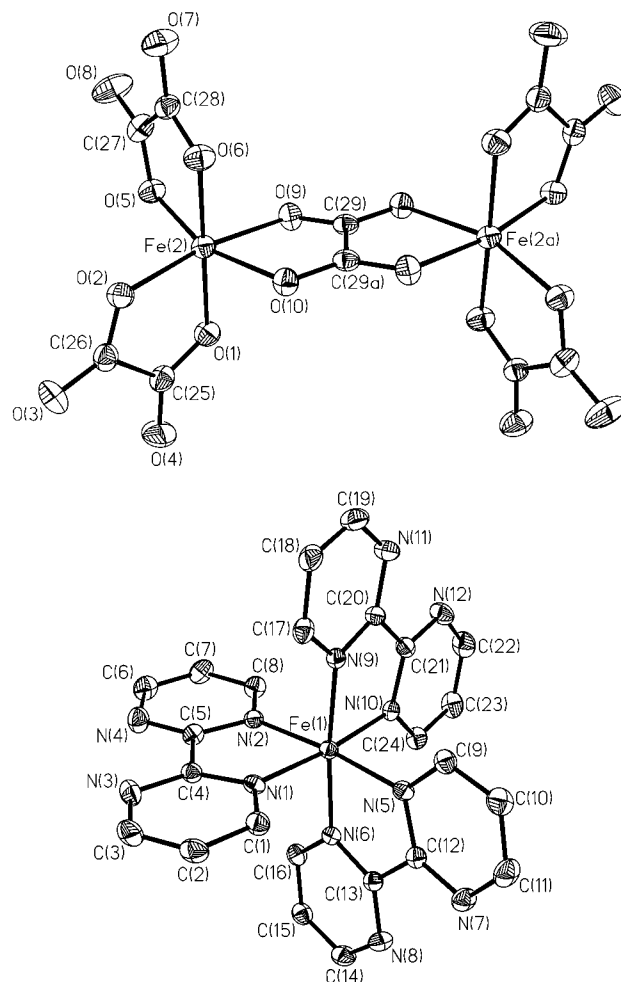


Figure 1. Perspective views of the structures of the dinuclear [Fe₂(ox)₅]⁴⁻ anion (top) and mononuclear [Fe(bpm)₃]²⁺ cation (bottom) occurring in complex **1**. Thermal ellipsoids are drawn at the 30% probability level.

defined by O(1), O(2), O(9), and O(6). The bridging oxalato is essentially planar because of the inversion center located at the midpoint of the C(29)–C(29a) bond, and the iron atom is 0.203-(1) Å out of this plane. The dihedral angles formed by the bridging and the two terminal oxalato groups are 83.3(1)° and 83.1(1)°. The distance between the two iron atoms through the bridging oxalato is 5.449(2) Å [Fe(2)···Fe(2a); a = symmetry code -*x*, -*y*, -*z*].

The [Fe(bpm)₃]²⁺ cation consists of the iron(II) ion coordinated to three bpm molecules in a distorted octahedral geometry (Figure 1, bottom). The average Fe(1)–N bond length is 1.978-(4) Å, a value that compares well with those reported for this unit in the compounds [Fe(bpm)₃]₂(ClO₄)₂·2H₂O (1.970(5) Å)⁴¹ and [Fe(bpm)₃]₂[Fe₂(N₃)₁₀]·2H₂O (1.972(4) Å),⁴² and that is in the range of the observed bond lengths for low-spin tris-chelated iron(II) complexes.^{5,43,44} The pyrimidyl rings are planar, as

(36) SHELXL PLUS, version 4.11/V; Bruker Analytical X-ray Instruments Inc.: Madison WI, 1990. SHELX NT, version 5.10; Bruker Analytical X-ray Instruments Inc.: Madison WI, 1998.

(37) Nardelli, M. *Comput. Chem.* **1983**, *7*, 95.

(38) Herpin, P. *Bull. Chem. Soc. Fr. Min. Crist.* **1958**, *81*, 245.

(39) Merrachi, E. H.; Mentzen, B. F.; Chassagneux, F.; Bouix, J. *Rev. Chim. Miner.* **1987**, *24*, 56.

(40) Merrachi, E. H.; Mentzen, B. F.; Chassagneux, F. *Rev. Chim. Miner.* **1987**, *24*, 427.

(41) De Munno, G.; Julve, M.; Real, J. A. *Inorg. Chim. Acta* **1997**, *255*, 185.

(42) De Munno, G.; Poerio, T.; Viau, G.; Julve, M.; Lloret, F. *Angew. Chem., Int. Ed. Engl.* **1997**, *36*, 1459.

(43) García Posse, M. E.; Juri, M. A.; Aymoning, P. J.; Piro, O. E.; Negri, H. A. *Inorg. Chem.* **1984**, *23*, 948.

(44) (a) Johansson, L.; Molund, M.; Oskarsson, A. *Inorg. Chim. Acta* **1978**, *31*, 117. (b) Fujiwara, T.; Iwamoto, E.; Yamamoto, Y. *Inorg. Chem.* **1984**, *23*, 115. (c) Cho, C. K.; Secco, A. *Acta Crystallogr., Sect. C* **1992**, *48*, 165. (d) Koh, L. L.; Xu, Y.; Hsieh, A. K. *Acta Crystallogr., Sect. C* **1994**, *50*, 884.

Table 2. Selected Bond Distances (Å) and Bond Angles (deg) for Compound 1

Distances					
Fe(1)–N(1)	1.983(3)	Fe(1)–N(2)	1.995(4)		
Fe(1)–N(5)	1.978(4)	Fe(1)–N(6)	1.971(4)		
Fe(1)–N(9)	1.976(5)	Fe(1)–N(10)	1.967(3)		
Fe(2)–O(1)	1.991(4)	Fe(2)–O(2)	1.967(3)		
Fe(2)–O(5)	1.971(4)	Fe(2)–O(6)	1.979(4)		
Fe(2)–O(9)	2.099(3)	Fe(2)–O(10)	2.085(4)		
Angles					
N(1)–Fe(1)–N(2)	81.4(2)	N(1)–Fe(1)–N(5)	93.8(2)		
N(2)–Fe(1)–N(5)	174.0(2)	N(1)–Fe(1)–N(6)	88.5(1)		
N(2)–Fe(1)–N(6)	94.6(2)	N(5)–Fe(1)–N(6)	81.6(2)		
N(1)–Fe(1)–N(9)	95.7(2)	N(2)–Fe(1)–N(9)	89.8(2)		
N(5)–Fe(1)–N(9)	94.3(2)	N(6)–Fe(1)–N(9)	174.4(2)		
N(1)–Fe(1)–N(10)	174.1(2)	N(2)–Fe(1)–N(10)	93.4(2)		
N(5)–Fe(1)–N(10)	91.5(2)	N(6)–Fe(1)–N(10)	94.9(2)		
N(9)–Fe(1)–N(10)	81.3(2)	O(1)–Fe(2)–O(2)	81.2(1)		
O(1)–Fe(2)–O(5)	102.1(2)	O(2)–Fe(2)–O(5)	98.4(2)		
O(1)–Fe(2)–O(6)	175.0(2)	O(2)–Fe(2)–O(6)	95.6(2)		
O(5)–Fe(2)–O(6)	82.1(2)	O(1)–Fe(2)–O(9)	89.4(1)		
O(2)–Fe(2)–O(9)	169.9(1)	O(5)–Fe(2)–O(9)	87.3(2)		
O(6)–Fe(2)–O(9)	93.4(1)	O(1)–Fe(2)–O(10)	90.6(2)		
O(2)–Fe(2)–O(10)	97.0(2)	O(5)–Fe(2)–O(10)	161.3(2)		
O(6)–Fe(2)–O(10)	85.9(2)	O(9)–Fe(2)–O(10)	79.2(1)		
Hydrogen Bonds ^b					
A	D	H	A...D	A...H–D	
O(13)	O(11)	H(1w)	2.79(1)	142(1)	
O(5)	O(11)	H(2w)	2.88(1)	141(1)	
O(8)	O(12)	H(4w)	2.88(1)	151(1)	
O(11)	O(14)	H(7w)	2.85(1)	165(1)	
O(4b) ^a	O(13)	H(5w)	2.94(1)	172(1)	

^a b = symmetry code 1 – x, –y, –z. ^b A = acceptor; D = donor.

expected, with deviations not greater than 0.016(5) Å for C(17) from the mean planes. The carbon–carbon and carbon–nitrogen bond lengths within the pyrimidyl rings agree with those observed in other iron(II) complexes with chelating bpm.^{41,42,45,46} The carbon–carbon bond lengths between the pyrimidyl rings [*av.* 1.477(7) Å] are somewhat shorter than those reported for the dinuclear iron(II) complexes [Fe₂(bpm)₃(NCS)₄] [1.510(11) and 1.502(14) Å for chelating and bridging bpm, respectively]⁴⁵ and [Fe₂(H₂O)₈(bpm)](SO₄)₂·2H₂O [1.488(4) Å].⁴⁷ The bpm ligand as a whole is almost planar [the dihedral angles between the pyrimidine rings are 1.7(1)°, 1.9(1)°, and 0.3(1)°]. The values of the dihedral angles between the bpm ligands are 83.0(1)°, 87.2(1)°, and 96.4(1)°. The shortest separation between low- and high-spin iron centers is 6.841(2) Å [Fe(1)···Fe(2b); b = symmetry code 1 + x, y, 1 + z], whereas that between the low-spin centers is 7.961(2) Å [Fe(1)···Fe(1c); c = symmetry code 2 – x, –y, 1 – z].

The dinuclear units are held together by means of H bonds involving some of the oxalato-oxygens [O(4), O(5), O(8)] and all crystallization water molecules (see end of Table 2). Noncovalent interactions are expected to occur in compounds containing π systems. In the case of compound 1, an examination of the relative geometric positions of the planar bpm ligands in the crystal structure shows that the tris-chelated cations are connected by off-set face-to-face interactions in such a way as to form a chain along the y axis. Only two of the three bpm molecules are involved in these stacking interactions within the

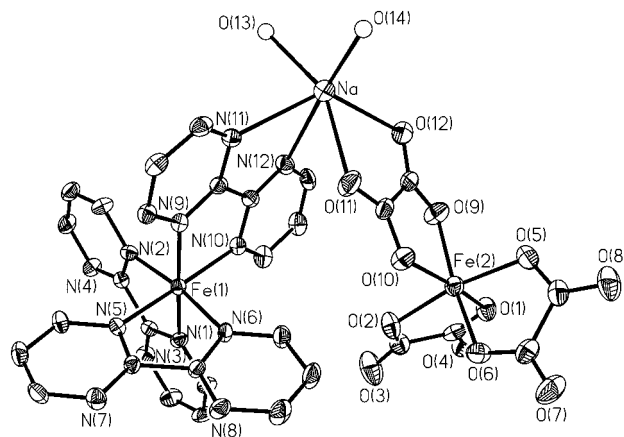


Figure 2. Perspective view of complex 2. Hydrogen atoms and uncoordinated water molecules have been omitted for clarity. Thermal ellipsoids are drawn at the 30% probability level.

chain, the distance between the mean planes planes C(1)–C(8), C(1c)–C(8c) and C(17)–C(24), C(17d)–C(24d) [d = symmetry code 2 – x, 1 – y, 1 – z] being 3.29(1) and 3.22(1) Å, respectively.

Fe(bpm)₃Na(H₂O)₂Fe(ox)₃·4H₂O (2). The structure of compound 2 consists of neutral trinuclear Fe(bpm)₃Na(H₂O)₂Fe(ox)₃ units (Figure 2) and crystallization water molecules linked by hydrogen bonds in which the water molecules and oxalato groups are involved.

The trinuclear entity contains tris-chelated [Fe(ox)₃]^{3–} and [Fe(bpm)₃]²⁺ units, which act as bidentate ligands through one oxalato ligand and a bpm group, respectively, toward a central sodium atom. The sodium atom is hexacoordinate; two nitrogen atoms of a bpm molecule, two oxygen atoms of an oxalato group, and two water molecules in *cis* positions build a highly distorted octahedral environment around the sodium atom, inasmuch as only the angle N(12)–Na–O(14) has a value of almost 180° [172.8°]. This distortion is mainly due to the position of the O(12) atom, which reduces the trans N(11)–Na–O(12) angle to 128.6° and increases the adjacent O(13)–Na–O(12) angle to 123.9°. The Na–O(water) distances [*av.* 2.34(1) Å] are similar to one Na–O(ox) [Na–O(12)], whereas the second one is longer [2.511(6) Å]. These values are in agreement with those reported for the oxalato-bridged two-dimensional [NaCr((bpm)(ox))·5H₂O] [*av.* 2.382(5) Å (Na–O(ox))]²⁸ and [NaCr(bpy)(ox)₂(H₂O)]·2H₂O [2.511(4)–2.331(4) Å (Na–O(ox)) and 2.371(5)–2.325(4) Å (Na–O(water))]⁴⁸ and for the three-dimensional [Fe(bpy)₃][NaFe(ox)₃] [*av.* 2.318(3) Å (Na–O(ox))],⁷ [Ni(bpy)₃][NaAl(ox)₃] [2.378(3) Å (Na–O(ox))],⁹ and [Cr(bpy)₃][NaCr(ox)₃]ClO₄ [2.320(6) Å (Na–O(ox))]¹² compounds. The Na–N distances vary from 2.55(1) to 2.68(1) Å, values that are somewhat greater than those observed in the compound [NaCr(bpm)(ox)]·5H₂O [2.489(4) Å for Na–N(bpm)].²⁸ The iron atoms in the cationic (Fe(1)) and anionic (Fe(2)) units are bound to three bpm (Fe(1)) and three oxalate (Fe(2)), both exhibiting distorted octahedral geometries. No remarkable differences were found in the Fe(1)–N and Fe(2)–O distances of the terminal and chelating bpm and ox groups. The average Fe(2)–O and Fe(1)–N bond lengths [2.009(6) and 1.977(6) Å, respectively] are similar to those found in 1 for terminal oxalato and bipyrimidine, respectively. Consequently, compound 2 contains a low-spin iron(II) (Fe(1)) and a high-spin iron(III) (Fe(2)) center.

(45) Real, J. A.; Zarembovitch, J.; Kahn, O.; Solans, X. *Inorg. Chem.* **1987**, 2939.

(46) Claude, R.; Real, J. A.; Zarembovitch, J.; Kahn, O.; Ouahab, L.; Grandjean, D.; Boukheddaden, K.; Varret, F.; Dworkin, A. *Inorg. Chem.* **1990**, 29, 4442.

(47) Andrés, E.; De Munno, G.; Julve, M.; Real, J. A.; Lloret, F. *J. Chem. Soc., Dalton Trans.* **1993**, 2169.

(48) Muñoz, M. C.; Julve, M.; Lloret, F.; Faus, J.; Andruh, M. *J. Chem. Soc., Dalton Trans.* **1998**, 3125.

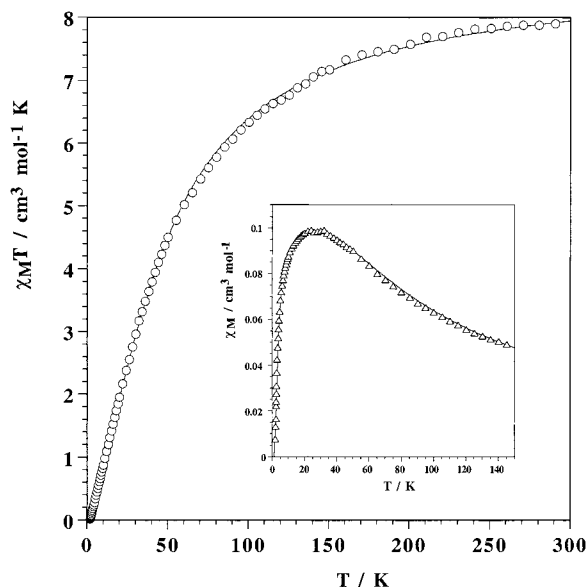


Figure 3. Thermal variation of $\chi_M T$ (○) and χ_M (△) for compound **1**. The solid line is the best fit (see text).

The pyrimidyl rings of the bpm ligands are planar, as expected, with deviations not greater than 0.013(9) Å for C(14) from the mean planes. The bpm ligands are not far from planarity [the dihedral angles between the pyrimidine rings are 1.8(2)°, 3.8(2)°, and 5.6(2)°]. The dihedral angles between the three bpm mean planes are 92.4(1)°, 91.7(1)°, and 90.9(1)°. The oxalate groups are also planar, and the dihedral angles they form with each other are 100.5(2)°, 75.7(2)°, and 80.3(2)°. The trinuclear units are held together by means of H bonds in which the oxygen atom O(8) of the oxalate group and a crystallization water molecule are involved [O(13)⋯O(8f) = 2.271(1) Å; f = symmetry code $-1 + x, y, z$]. The resulting chain propagates along the *x* axis. Adjacent chains are joined in the *xy* plane by hydrogen bonds occurring between the O(3) oxalate atom and the O(14g) crystallization water molecule [O(14g)⋯O(3) = 2.93(2) Å; g = symmetry code $-x, -0.5 + y, 0.5 - z$].

The separation between the Fe(1) and Fe(2) centers in the trinuclear unit is 6.763(2) Å, a value much shorter than the intermolecular distances between low-spin [8.152(2) Å for [Fe(1)⋯Fe(1e)]; e = symmetry code $x, -0.5 - y, -0.5 + z$] and high-spin [8.992(2) Å for [Fe(2)⋯Fe(2d)]; d = $-1 - x, -1 - y, -z$] centers.

Magnetic Properties of 1. The magnetic behavior of complex **1** is shown in Figure 3 in the form of a $\chi_M T$ vs *T* plot (χ_M is the magnetic susceptibility per two iron(III) ions). At room temperature, the value of $\chi_M T$ is 7.93 cm³ mol⁻¹ K. This value, which is somewhat smaller than that calculated for two uncoupled high-spin Fe(III) ions [8.75 cm³ mol⁻¹ K with *g* = 2.0], decreases rapidly on cooling and becomes practically zero at 2.0 K. These features and the presence of a maximum in the susceptibility curve at 27 K (see inset of Figure 3) demonstrate that a relatively strong antiferromagnetic coupling between the iron(III) ions through the bridging oxalato occurs in **1**. Taking into account its dinuclear nature, we have treated the magnetic data using the appropriate expression derived from the isotropic Hamiltonian:

$$\hat{H} = -J\hat{S}_1 \cdot \hat{S}_2 + g\beta H(\hat{S}_1 + \hat{S}_2) \quad (1)$$

where *J* is the exchange coupling parameter, \hat{S}_1 and \hat{S}_2 are the spin operators associated with the local spins $S_1 = S_2 = 5/2$, and *g* is the Landé factor. Best-fit parameters of the magnetic

Table 3. Selected Bond Distances (Å) and Bond Angles (deg) for Compound **2**

Distances			
Fe(1)–N(1)	1.972(4)	Fe(1)–N(2)	1.970(5)
Fe(1)–N(5)	1.970(4)	Fe(1)–N(6)	1.977(4)
Fe(1)–N(9)	1.992(4)	Fe(1)–N(10)	1.989(4)
Na–N(11)	2.547(6)	Na–N(12)	2.675(6)
Na–O(11)	2.511(6)	Na–O(12)	2.374(6)
Na–O(13)	2.363(9)	Na–O(14)	2.345(12)
Fe(2)–O(1)	2.010(4)	Fe(2)–O(2)	2.031(5)
Fe(2)–O(6)	1.992(5)	Fe(2)–O(5)	1.996(5)
Fe(2)–O(9)	2.006(5)	Fe(2)–O(10)	2.015(4)
Angles			
N(1)–Fe(1)–N(2)	81.5(2)	N(1)–Fe(1)–N(5)	91.3(2)
N(1)–Fe(1)–N(6)	93.1(2)	N(1)–Fe(1)–N(10)	93.8(2)
N(1)–Fe(1)–N(9)	174.0(2)	N(2)–Fe(1)–N(5)	93.5(2)
N(2)–Fe(1)–N(6)	172.3(2)	N(2)–Fe(1)–N(9)	95.0(2)
N(5)–Fe(1)–N(10)	174.3(2)	N(2)–Fe(1)–N(10)	89.9(2)
N(5)–Fe(1)–N(6)	81.1(2)	N(6)–Fe(1)–N(10)	96.0(2)
N(5)–Fe(1)–N(9)	93.8(2)	N(6)–Fe(1)–N(9)	90.8(2)
N(10)–Fe(1)–N(9)	81.3(2)	O(14)–Na–O(13)	103.0(4)
O(14)–Na–O(12)	103.3(4)	N(11)–Na–N(12)	64.9(2)
O(13)–Na–O(12)	123.9(3)	O(14)–Na–O(11)	94.1(3)
O(13)–Na–O(11)	154.3(3)	O(12)–Na–O(11)	69.0(2)
O(14)–Na–N(11)	111.5(3)	O(13)–Na–N(11)	83.9(3)
O(12)–Na–N(11)	128.6(2)	O(11)–Na–N(11)	71.9(2)
O(14)–Na–N(12)	172.3(3)	O(13)–Na–N(12)	83.7(3)
O(12)–Na–N(12)	75.6(2)	O(11)–Na–N(12)	78.4(2)
O(1)–Fe(2)–O(2)	80.4(2)	O(5)–Fe(2)–O(1)	93.8(2)
O(6)–Fe(2)–O(1)	97.2(2)	O(6)–Fe(2)–O(5)	80.8(2)
O(6)–Fe(2)–O(9)	166.4(2)	O(5)–Fe(2)–O(9)	89.8(2)
O(9)–Fe(2)–O(1)	93.2(2)	O(6)–Fe(2)–O(10)	90.8(2)
O(5)–Fe(2)–O(10)	98.2(2)	O(9)–Fe(2)–O(10)	80.8(2)
O(1)–Fe(2)–O(10)	166.6(2)	O(6)–Fe(2)–O(2)	91.9(2)
O(5)–Fe(2)–O(2)	170.1(2)	O(9)–Fe(2)–O(2)	98.5(2)
O(10)–Fe(2)–O(2)	88.6(2)		

data of **1** are *J* = –6.6 cm⁻¹, *g* = 2.0, and *R* = 2.1 × 10⁻⁵ (*R* is the agreement factor defined as $\sum_i [(\chi_M)_{\text{obs}}(i) - (\chi_M)_{\text{calc}}(i)]^2 / \sum_i [(\chi_M)_{\text{obs}}(i)]^2$). The calculated curve matches the magnetic data very well, as indicated by the low value of *R*. In the case of complex **2**, the value of the magnetic moment at room temperature ($\mu_{\text{eff}} = 5.91 \mu_B$) is as expected for a high-spin iron(III) complex and is in agreement with its crystal structure.

It should be noted that as far as we are aware, **1** is the first structurally characterized example of an oxalato-bridged dinuclear iron(III) complex. The value of the antiferromagnetic coupling in **1** (–6.6 cm⁻¹) shows once more the special ability of the oxalato bridge to mediate quite strong magnetic interactions between paramagnetic centers, which are separated by more than 5 Å.^{18–21} The magnetic coupling in **1** compares well with that previously reported for the assumed oxalato-bridged compounds [Fe₂(acac)₄(ox)]·1/2H₂O (acac = acetylacetonate) (*J* = –7.22 cm⁻¹),⁴⁹ [Fe₂(phen)₄(ox)]Cl₄ (phen = 1,10-phenanthroline) (*J* = –6.8 cm⁻¹),⁵⁰ and [Fe₂(salen)₂(ox)]·H₂O (salen = *N,N'*-ethylenebis(salicylideneamine)) (*J* = –7.1 cm⁻¹),⁵¹ whose structures are unknown.

There are several interesting aspects that emerge from the present work. The first concerns the synthetic possibilities arising from the use of the tris-chelated low-spin [Fe(bpm)₃]²⁺ cation. Recently, its use as a cation has allowed us to prepare single crystals of the ferromagnetically coupled [Fe₂(N₃)₁₀]⁴⁺ dinuclear iron(III) complex.⁴² Here, it provides us with two different compounds: the exotic dinuclear entity [Fe₂(ox)₅]⁴⁺ in **1** where oxalato plays both terminal and bridging roles and the neutral

(49) Julve, M.; Kahn, O. *Inorg. Chim. Acta* **1983**, *76*, L39.

(50) Wroblewski, J. T.; Brown, D. B. Unpublished results.

(51) Lloret, F.; Julve, M.; Faus, J.; Solans, X.; Journaux, Y.; Morgenstern-Badarau, I. *Inorg. Chem.* **1990**, *29*, 2232.

Table 4. Selected Magneto-Structural Data for the Oxalato-Bridged Complexes $[\text{M}_2(\text{ox})_5]^{(2n-10)+}$

M	M–O(bridge) ^a /Å	M···M ^b /Å	$-J^c/\text{cm}^{-1}$	$-n^2J^d/\text{cm}^{-1}$	ref
Ni(II)	2.072(4)	5.380(2)	22.8	91.2	21
Cr(III)	2.035(7)	5.32	6.2	55.8	32
Fe(III)	2.092(4)	5.449(2)	6.6	165	this

work

^a Average value of the metal-to-bridging-oxalato bond length. ^b Metal–metal separation through bridging oxalato. ^c Value of the exchange coupling with the Hamiltonian defined as $\hat{H} = -J\hat{S}_1\cdot\hat{S}_2$. ^d n is the number of unpaired electrons on each metal ion M.

trinuclear complex **2** through self-assembly via sodium(I). The tris-chelated iron(II) complex acts as a cation in the former compound, whereas it acts as a bidentate ligand toward sodium(I) in the latter. The second point that deserves to be pointed out is the fact that the parent Ni(II)²¹ and Cr(III)³² derivatives of the anionic entity of **1** were known, the cations being H₃-dien³⁺ (dien = diethylenetriamine) and NBu₄⁺ (*n*-tetrabutylammonium), respectively. So these species cannot be considered uncommon, and in the near future this family could be extended to other transition metal ions. Finally, the most interesting point concerning this family of complexes is the opportunity that their magneto-structural characterization provides a comparison of the efficiency of the σ and π exchange pathways through the bridging oxalato. The relevant magneto-structural data are listed in Table 4. Given that the number of unpaired electrons on the metal ion in this series is different, the value of the coupling to be compared is n^2J instead of J .⁵² The experimental n^2J value can be decomposed into a sum of individual contributions, $J_{\mu\nu}$, involving each pair of magnetic orbital involved in the exchange phenomenon:

$$n^2J = \sum_{\mu=1}^n \sum_{\nu=1}^n J_{\mu\nu} \quad (2)$$

If the x and y axes are defined as the metal-to-bridging-oxalato bonds, it is clear that in the case of the nickel(II) dimer only the σ exchange pathway is operative:

$$-91.2 \text{ cm}^{-1} = J_{x^2-y^2, x^2-y^2} + J_{d_z^2, d_z^2} + 2J_{x^2-y^2, d_z^2} \quad (3)$$

The first two terms in eq 3 are negative (antiferromagnetic contributions), whereas the last one is positive (ferromagnetic contribution because of the strict orthogonality between the $d_{x^2-y^2}$ and d_{z^2} magnetic orbitals from the two metal ions). Because of the better overlap, the first term in eq 3 is more important than the second.²¹ In addition, given that the ferromagnetic coupling decreases as the length of the bridge increases,⁵³ the last term in this equation is expected to be weak. In the chromium(III) dimer, only the π exchange pathway is operative, (Cr(III) in O_h symmetry is a t_{2g}^3 system). The value of n^2J in this compound (-55.8 cm^{-1}) is close to that of the nickel(II) dimer and reveals

that the purely π pathway through oxalato is also very efficient. Given that in the iron(III) dimer (**1**) the two exchange pathways are operative (Fe(III) in O_h symmetry), one would expect a maximum value of $n^2J = -(91.2 + 55.8) = -147 \text{ cm}^{-1}$ for this compound. The experimental antiferromagnetic coupling in **1** (-165 cm^{-1}) is close but somewhat larger. The consideration of the ferromagnetic terms arising from the orthogonal interaction between d_{π} and d_{σ} in **1** would decrease the calculated value of $-n^2J$, resulting in a larger gap between the experimental and calculated n^2J values. In our approach, we have neglected the ferromagnetic contributions through the bridging oxalato because they are expected to be weak for extended bridges.⁵³ The fact that the experimental value of $-n^2J$ for **1** is somewhat greater than the calculated one is most likely due to the combination of two factors that enhance the antiferromagnetic coupling through both σ and π pathways in the case of the Fe(III) derivative: (i) first, the greater covalency of the Fe(III)–O(ox) bonds and thus the better overlap; (ii) second, the smaller energy gap between the SOMO's of the Fe(III) ion and the symmetry-adapted HOMO's of the oxalate. A quite comprehensive discussion of the influence of orbital and structural parameters on the magnetic coupling in oxalato-bridged copper(II) complexes (only the σ pathway and one unpaired electron per metal center being involved) was published recently.⁵⁴ In the present case, more experimental work is needed to complete Table 4 with additional examples concerning other first-row transition metal ions. A further theoretical study of the whole family of homodinuclear species would provide a clear picture of the contribution of the different terms involved in the exchange pathways through the bridging oxalato.

Note Added in Proof: When correcting these proofs, we were aware of two recent publications concerning the magnetostructural investigation of three compounds of similar nature containing the oxalato-bridged $[\text{Fe}_2(\text{ox})_5]^{4-}$ anion and tetrathiafulvalene derivatives as cations.^{55,56} The antiferromagnetic coupling between the iron(III) ions across bridging oxalato in them is found to vary in the range -6.9 to -7.4 cm^{-1} , in good agreement with the value reported for complex **1** in the present work.

Acknowledgment. Financial support from the Spanish DGICYT (Project PB97-1397), the Italian Ministero dell'Università e della Ricerca Scientifica e Tecnologica, and the Human Capital and Mobility Program (Network on Magnetic Molecular Materials from EEC) through Grant ERBCHRX-CT920080 is gratefully acknowledged.

Supporting Information Available: X-ray crystallographic files in CIF format. This material is available free of charge via the Internet at <http://pubs.acs.org>.

IC000258Q

(52) Kahn, O. *Struct. Bonding (Berlin)* **1987**, 68, 89.(53) Kahn, O. *Comments Inorg. Chem.* **1984**, 3, 105.(54) Cano, J.; Alemany, P.; Alvarez, S.; Verdager, M.; Ruiz, R. *Chem.–Eur. J.* **1998**, 4, 476.(55) Coronado, E.; Galán-Mascarós, J. R.; Gómez-García, C. J. *J. Chem. Soc., Dalton Trans.* **2000**, 205.(56) Rashid, S.; Turner, S. S.; Day, P.; Light, M. E.; Hursthouse, M. B. *Inorg. Chem.* **2000**, 39, 2426.